9

Physiological Pharmacokinetic Models

Pharmacokinetic models are developed to describe and predict the time course of drugs and/or related chemicals throughout the body. The classical approaches, introduced in Chaps. 1 and 2, lead to the elaboration of compartmental models which often have important clinical applications, particularly in the development of dosage regimens. However, these models are inherently limited in the amount of information they provide because, in the usual case, the compartments and the parameters have no obvious relationship to anatomical structure or physiological function of the species under study. The introduction of clearance concepts (outlined in Chap. 8) to pharmacokinetic models represents an enormous step toward bridging the gap between mathematical description and physiological reality but still results in an incomplete picture.

In recent years efforts have been directed toward the development of physiologically realistic pharmacokinetic models. These detailed models are elaborated on the basis of the known anatomy and physiology of humans or other animals and incorporate physiological, anatomical, and physiochemical data. The history of this development and the applications have recently been reviewed by Himmelstein and Lutz [1].

In principle, these comprehensive models are superior to classical compartment models in several respects. Ideally, they provide an exact description of the time course of drug concentration in any organ or tissue and are therefore able to provide greater insight to drug distribution in the body. Also, since the parameters of these models correspond to actual physiological and anatomical measures, such as organ blood flows and volumes, changes in the disposition kinetics of drug because of physiological or pathological alterations in body function may be predicted by perturbation of the appropriate parameter(s) [2]. Finally, these models introduce the possibility of animal scale-up which would provide a rational basis for the correlation of drug data among animal species [3].

A physiological pharmacokinetic model is composed of a series of lumped compartments (body regions) representing organs or tissue spaces whose drug concentrations are assumed to be uniform. The compartments are arranged in a flow diagram as illustrated by the general example in Fig. 9.1. The first step in the development of a physiological pharmacokinetic model is the selection of compartments to be included. An excellent discussion of this selection process has been presented by Bischoff [4], who notes that there is no simple way

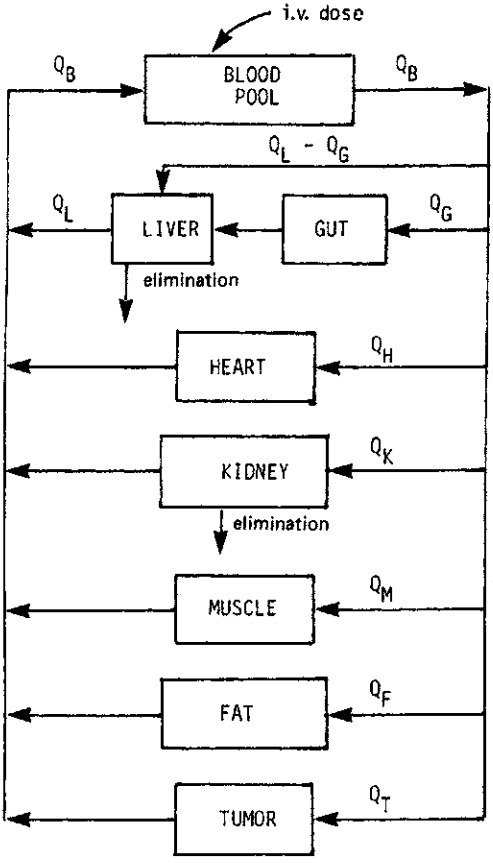

Fig. 9.1 Schematic representation of different regions of the body arranged in a flow diagram which constitutes a physiological pharmacokinetic model. The term Q denotes blood flow rate to a region. Subscripts are as follows: B, blood; L, liver; G, gut; H, heart; K, kidney; M, muscle; F, fat; T, tumor. In this particular model the liver and kidney are eliminating compartments.

to describe which body regions should be included and which might be excluded, since judgment is required as to the important aspects of the drug distribution events. An initial choice is made based on the pharmacodynamic, pharmacokinetic, and physiochemical characteristics of the drug as well as the anatomy and physiology of the body. Clearly, we wish to include body regions in which the drug exerts a pharmacologic or toxicologic effect. We must include organs that are involved in the elimination of the drug. It makes sense to include tissues or fluids that are easily sampled and tissue spaces that contain relatively large amounts of the drug.

Once the selection has been made, the kinds of information required by the model can be classified as (1) anatomical (e.g., organ and tissue volumes), (2) physiological (e.g., blood flow rates and enzyme reaction parameters), (3) thermodynamic (e.g., drug-protein binding isotherms), and (4) transport (e.g., membrane permeabilities). Rarely will all this information be needed for a specific model. We can often ignore transport and we can frequently express enzyme reaction and binding parameters in simple terms.

Body regions can usually be viewed as consisting of a large number of a single type of cell randomly distributed in the interstitial fluid and supplied with blood by a capillary. This representation is often further simplified, as shown in Fig. 9.2, by subdividing the region into three homogeneous fluid compartments: the capillary blood volume, the interstitial water, and the intracellular space. Most physiological pharmacokinetic models developed to data are based on the assumption that drug movement within a body region is much more rapid than the rate of delivery of drug to the region by the perfusing blood. In other words, exchange of drug between capillary blood and interstitial water

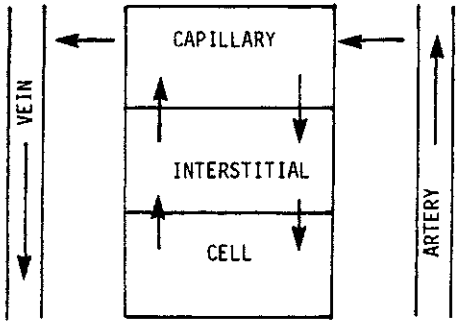

Fig. 9.2 Model for blood perfusion of local tissue region. Often, drug transport between capillary blood and interstitial space and between interstitial space and intracellular space is a very fast process compared to the rate of blood perfusion. Under these conditions the entire region may be considered as a lumped compartment (see Fig. 9.1).

is considered to be very rapid and the cell membrane is considered to be very permeable to the drug. In this case the concentration of a drug in the emergent (venous) blood from a tissue region is in equilibrium with that in the tissue. In effect, drug distribution into various body regions is rate limited by blood flow and specific regions can be represented by a single compartment as shown in Fig. 9.1. The assumption of perfusion-limited transport is applicable to relatively low molecular weight, weakly ionized, lipid-soluble drugs for which diffusion and movement across lipoidal membranes should be relatively rapid. On the other hand, membrane transport can be a slow step in the overall uptake of very polar, highly ionized, or charged drugs.

BLOOD FLOW RATE-LIMITED MODELS

All blood flow rate-limited physiological pharmacokinetic models are basically similar to the one shown in Fig. 9.1. Differential mass balance equations are written for each compartment to describe the inflow, outflow, accumulation, and disappearance of drug, and are solved simultaneously with the aid of a computer. The equations for this model can be derived using an approach suggested by Rowland et al. [5]. However, it is convenient to first examine a simpler model (Fig. 9.3A) and to consider separately drug distribution to a non-eliminating region such as the muscle (Fig. 9.3B) and to an eliminating region such as the liver (Fig. 9.3C).

The rates of change of *total concentration* of drug in the blood C_B and in the muscle C_M as a function of time for the model shown in Fig. 9.3B are

$$V_B \frac{dC_B}{dt} = Q_M C_o - Q_M C_i \tag{9.1}$$

and

$$V_M \frac{dC_M}{dt} = Q_M C_i - Q_M C_o \tag{9.2}$$

where V_B and V_M are volumes of the blood and muscle compartments, respectively; Q_M is blood flow to the muscle; and C_i and C_o are drug concentrations in blood entering and leaving the muscle compartment, respectively. The drug concentration in afferent blood C_i is equivalent to arterial blood concentration C_B. The drug concentration in efferent blood C_o, however, is equivalent to C_M only if there is no drug binding in the system or if binding is the same in blood and muscle. If this is not the case, then

$$C_o = \frac{C_M}{R_M} \tag{9.3}$$

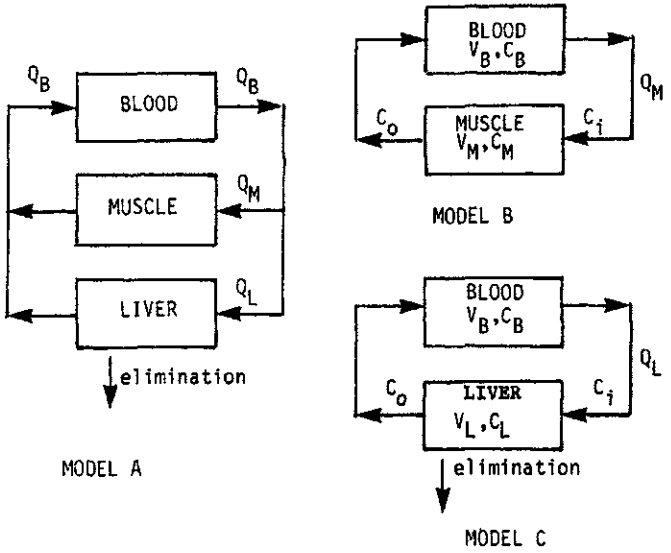

Fig. 9.3 Some simple flow models consisting of blood pool, noneliminating compartment, and eliminating compartment (model A), blood pool and noneliminating compartment (model B), and blood pool and eliminating compartment (model C). The terms Q, V, and C denote blood flow rate to a given region, anatomical volume of a region, and drug concentration, respectively. Subscripts indicate blood (B), muscle (M), and liver (L). The terms C_i and C_o signify drug concentrations in afferent (arterial) and efferent (venous) blood, respectively. In model A, $Q_B = Q_M + Q_L$.

where R_M is a partition coefficient relating total drug concentration in the tissue to total drug concentration in the venous blood at equilibrium. Since the total drug concentration in a compartment is equal to the free concentration divided by the fraction free, and since the concentration of free drug is assumed to be the same in all compartments, R_M is also given by

$$R_M = \frac{f_B}{f_M} \tag{9.4}$$

where f_B is the fraction free (unbound) of drug in the blood and f_M is the fraction free in the muscle.

It follows that (9.1) and (9.2) may be expressed as

$$V_B \frac{dC_B}{dt} = Q_M \frac{C_M}{R_M} - Q_M C_B \tag{9.5}$$

and

$$V_M \frac{dC_M}{dt} = Q_M \left(C_B - \frac{C_M}{R_M} \right) \tag{9.6}$$

The differential equations applying to drug distribution to an eliminating compartment (Fig. 9.3C), assuming that elimination rate is a function of free drug concentration in the compartment, are

$$V_B \frac{dC_B}{dt} = Q_L C_o - Q_L C_i \tag{9.7}$$

and

$$V_L \frac{dC_L}{dt} = Q_L C_i - Q_L C_o - Cl'_L C'_L \tag{9.8}$$

where C_L and C'_L are total and free drug concentrations in the liver, respectively, and Cl'_L is the intrinsic clearance with respect to free drug concentration in the liver.

Expressing C_i and C_o in (9.7) and (9.8) in terms of total drug concentrations in the respective compartments, we obtain

$$V_B \frac{dC_B}{dt} = Q_L \frac{C_L}{R_L} - Q_L C_B \tag{9.9}$$

and

$$V_L \frac{dC_L}{dt} = Q_L \left(C_B - \frac{C_L}{R_L} \right) - Cl'_L C'_L \tag{9.10}$$

where R_L is the equilibrium distribution ratio of drug between the liver and the emergent venous blood.

The free drug concentration in the liver is given by

$$C'_L = f_L C_L \tag{9.11}$$

where f_L is the free fraction of drug in the liver. The free fraction in the liver can be expressed in terms of the free fraction in the blood as follows [see Eq. (9.4)]:

$$f_L = \frac{f_B}{R_L} \tag{9.12}$$

Thus we may write (9.10) as

$$V_L \left(\frac{dC_L}{dt} \right) = Q_L \left(C_B - \frac{C_L}{R_L} \right) - \frac{f_B Cl'_L C_L}{R_L} \tag{9.13}$$

The elimination rate term on the right hand side of (9.10) or (9.13) results from the assumption that the rate of elimination is a function of free drug concentration in the elimination compartment. Most reports concerning blood flow rate-limited physiologically based pharmacokinetic models [3,4] have expressed this term as $Cl_L C_L/R_L$; this condition prevails when either $f_B = 1$ or the rate of drug elimination is a function of total drug concentration in the emergent venous blood (C_o or C_L/R_L). Rowland et al. [5] express this term as $Cl_L C_L$; this condition prevails when either $f_L = 1$ or the elimination rate is a function of total drug concentration in the eliminating compartment.

The appropriate differential equations describing the more complete model in Fig. 9.3A may be deduced by considering Eqs. (9.5), (9.6), (9.9), and (9.10). It follows that

$$V_B \frac{dC_B}{dt} = Q_M \frac{C_M}{R_M} + Q_L \frac{C_L}{R_L} - Q_B C_B \tag{9.14}$$

$$V_M \frac{dC_M}{dt} = Q_M \left(C_B - \frac{C_M}{R_M} \right) \tag{9.15}$$

and

$$V_L \frac{dC_L}{dt} = Q_L \left(C_B - \frac{C_L}{R_L} \right) - Cl'_L C'_L \tag{9.16}$$

or

$$V_L \frac{dC_L}{dt} = Q_L \left(C_B - \frac{C_L}{R_L} \right) - \frac{f_B Cl'_L C_L}{R_L} \tag{9.17}$$

It can now be appreciated that the task of writing the differential equations for a model as complex as that in Fig. 9.1 is relatively straightforward. The mass-balance rate equation for total drug concentration in a noneliminating compartment such as the heart, muscle, fat, or tumor region is given by an equation similar to (9.15). The mass-balance rate equation for a compartment that metabolizes, excretes, or otherwise eliminates the drug must also contain a term to account for elimination [see (9.16)]. The liver compartment of the model shown in Fig. 9.1 is a more accurate representation of the mammalian anatomy. Total drug concentration as a function of time for this model is given by

$$V_L \frac{dC_L}{dt} = (Q_L - Q_G) C_B + Q_G \frac{C_G}{R_G} - Q_L \frac{C_L}{R_L} - Cl'_L C'_L \tag{9.18}$$

where it is assumed that elimination is a first-order (linear) process and is a function of free drug concentration in the liver (i.e., C_L'). The subscripts denote liver (L), gastrointestinal tract (G), and blood (B). The mass-balance rate equation for drug in the blood pool is given by

$$V_B \frac{dC_B}{dt} = Q_L \frac{C_L}{R_L} + Q_H \frac{C_H}{R_H} + Q_K \frac{C_K}{R_K} + Q_M \frac{C_M}{R_M} + Q_F \frac{C_F}{R_F} + Q_T \frac{C_T}{R_T} - Q_B C_B \tag{9.19}$$

where the subscripts denote heart (H), kidney (K), muscle (M), fat (F), and tumor (T).

The addition of other body regions to the model usually presents few difficulties. For each new compartment, we must add an additional mass-balance rate equation [such as (9.15) or (9.16)] to the series as well as an additional term [i.e., $Q_t(C_t/R_t)$, where t refers to the new compartment] to the equation describing drug concentration in the blood pool [e.g., (9.19)]. The incorporation of the lung in a physiological pharmacokinetic model is somewhat more complicated because of its anatomical position (see Fig. 9.4). In this case the mass-balance rate equation for drug in the blood pool is given by

$$V_B \frac{dC_B}{dt} = Q_{Lu} \frac{C_{Lu}}{R_{Lu}} - Q_B C_B \tag{9.20}$$

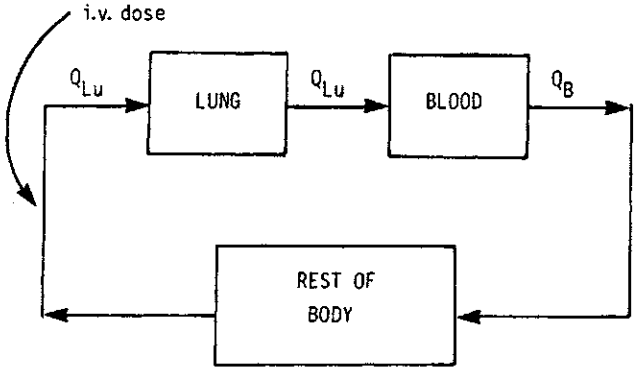

Fig. 9.4 Blood flow model showing the anatomical position of the lung relative to the site of intravenous drug administration. Q denotes blood flow rate. The subscripts refer to the lung (Lu) and blood (B). $Q_{Lu} = Q_B$. (Data from Ref. 14.)

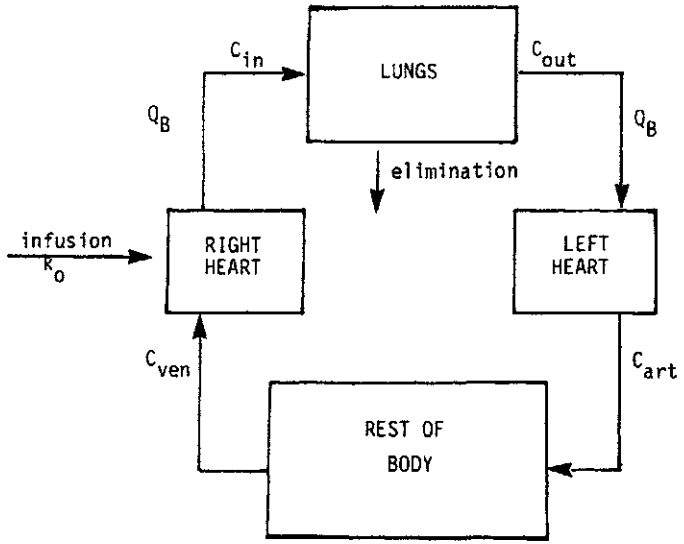

Fig. 9.5 Blood flow model showing the anatomical position of the lung relative to the site of intravenous drug administration, venous blood, and arterial blood. The model assumes that drug is given by intravenous infusion at a constant rate equal to k_0. C_{in} and C_{out} are drug concentrations in afferent and efferent blood perfusing the lung. Q_B denotes total blood flow rate (cardiac output). C_{art} and C_{ven} are drug concentrations in the arterial and venous blood pool. (Data from Ref. 18.)

and that for drug in the lung is given by

$$V_{Lu}\frac{dC_{Lu}}{dt} = \sum\left(Q_t\frac{C_t}{R_t}\right) - Q_{Lu}\frac{C_{Lu}}{R_{Lu}} \qquad (9.21)$$

where the subscript Lu denotes the lung and the summation term applies to all other compartments (except the blood pool) in the model. As indicated in Fig. 9.4, $Q_{Lu} = Q_B$.

The input function (dosing) for the model is usually handled by a programming step. For example, an intravenous bolus dose or relatively short intravenous infusion is introduced as an initial condition for the blood pool, while the initial condition for the amount of drug in all other compartments is set at zero. This approach works well in most situations. An exception is the case where drug is eliminated by the lung, particularly when lung clearance is significant compared to blood flow rate. In this situation one should probably split the blood pool into a venous pool and arterial pool (see Fig. 9.5) and program the initial condition for the venous pool. Since this model is

different from that shown in Fig. 9.1 or 9.4, a different set of differential equations is required.

EXPERIMENTAL CONSIDERATIONS

The blood flow rates and tissue volumes required to solve the differential equations may be determined experimentally, but this is rarely done. Typically, one employs average values that are appropriate for size and animal species. A listing of volumes and blood flow rates of different body regions for a standard man (70 kg body weight, 1.83 m^2 surface area, 30 to 39 years) is presented in Table 9.1. Values for other species, including the dog [6–8], the rat [9–11], the mouse [7,11,12], and the monkey [7,11,13], are available in the biomedical literature. Some investigators have developed scaling relations for organ volumes as a function of mammal body weight [11].

Although there is general agreement that R values must be determined experimentally for a specific drug, a value determined in one species may not apply to a second species. There is also some

Table 9.1 Volumes and Blood Flow Rates of Different Body Regions for a Standard Man

Tissue	Volume (liters)	Blood Flow Rate (ml/min)
Blood	5.4	–
Arterial	1.4	–
Venous	4.0	–
Plasma	3.0	–
Muscle	30.0	1200
Kidneys	0.3	1250
Liver	1.5	1500
Heart	0.3	240
Gastrointestinal tract	2.4	1200
Fat	10.0	200
Lung	0.6	–
Brain	1.5	750

Note: Characteristics of the standard man are: 70 kg body weight, 1.83 m^2 surface area, 30 to 39 years of age, and cardiac output of 5600 ml/min.

confusion as to the appropriate method of determining the tissue-to-blood partition coefficient of a drug. Some investigators have made measurements after a single bolus dose of a drug, whereas others have determined the distribution ratio only after infusing the drug to steady state. Chen and Gross [14] have discussed the difficulty in relating R values to partition coefficients determined after a single dose. They clearly show that, in general, R values for both eliminating and noneliminating tissues should be calculated from distribution ratios determined at steady state. A distribution ratio determined some time after a single bolus dose of a drug will approximate the R value in a noneliminating tissue only for drugs with relatively long half-lives [14]. The same may not be true in an eliminating tissue.

The tissue-to-blood distribution ratio determined at steady state is equivalent to the R value for any noneliminating tissue or compartment. This may be seen by considering Eq. (9.15) at steady state. Under these conditions the differential term is equal to zero and the equation may be rearranged to yield

$$R_M = \frac{C_M^{ss}}{C_B^{ss}} \tag{9.22}$$

where the superscript ss denotes steady state.

The situation is more complex in an eliminating compartment. The steady-state ratio of drug concentration in tissue to that in blood for a tissue that eliminates the drug will always underestimate the R value. This may be seen by considering Eq. (9.16) at steady state. Under these conditions the equation reduces to

$$Q_L C_B^{ss} - Q_L \frac{C_L^{ss}}{R_L} - Cl'_L C_L^{ss} = 0 \tag{9.23}$$

or [according to Eq. (9.17)]

$$Q_L C_B^{ss} - Q_L \frac{C_L^{ss}}{R_L} - \frac{f_B Cl'_L C_L^{ss}}{R_L} = 0 \tag{9.24}$$

Rearranging terms and solving for R_L yields

$$R_L = \frac{C_L^{ss}}{C_B^{ss}} \frac{Q_L + f_B Cl'_L}{Q_L} \tag{9.25}$$

If the effective intrinsic clearance is much smaller than organ blood flow rate, the steady-state distribution ratio will approximate the R value. If this is not the case, $R_L > C_L^{ss}/C_B^{ss}$. Large errors are

encountered for drugs with high effective intrinsic clearances relative to organ blood flow rate. In these cases R values must be calculated based on both steady-state distribution ratios and estimates of organ blood flow rates, as indicated by Eq. (9.25).

BLOOD CLEARANCE

Drug clearance from the blood is defined as the intravenous dose divided by the total area under the drug concentration in blood versus time curve. Consider the model shown in Fig. 9.3A. Solving Eqs. (9.14), (9.15), and (9.17) simultaneously for C_B, integrating the resulting triexponential equations from $t = 0$ to $t = \infty$, and dividing the dose by this area yields

$$Cl_B = \frac{Q_L f_B Cl'_L}{Q_L + f_B Cl'_L} \tag{9.26}$$

which is the familiar expression for clearance proposed by Wilkinson and Shand [15]. Equation (9.26) indicates for a drug such as indocyanine green with a relatively high effective intrinsic clearance (i.e., $f_B Cl'_L >> Q_L$) that drug clearance from the blood approximates liver blood flow, whereas for a drug with a relatively low effective intrinsic clearance (i.e., $Q_L >> f_B Cl'_L$), drug clearance from the blood approximates effective intrinsic clearance and is proportional to the fraction free in the blood, f_B.

If we were to assume that the elimination rate was a function of the total drug concentration in the emergent venous blood of the eliminating orgen, Eq. (9.26), which defines blood clearance, would take the form

$$Cl_B = \frac{Q_L Cl_L}{Q_L + Cl_L} \tag{9.27}$$

This equation indicates that drug clearance from the blood is independent of drug binding in the blood, which is inconsistent with considerable evidence from various systems that demonstrates, for drugs with relatively low effective intrinsic clearance, a marked dependence of Cl_B on plasma protein binding.

On the other hand, if we assume that elimination rate is a function of total drug concentration in the liver, we must redefine (9.26) as follows:

$$Cl_B = \frac{Q_L R_L Cl_L}{Q_L + R_L Cl_L} \tag{9.28}$$

For a drug with a low effective intrinsic clearance,

$$Cl_B \simeq R_L Cl_L = \frac{f_B Cl_L}{f_L} \tag{9.29}$$

Equation (9.28) differs from (9.26) by indicating for drugs with a low effective intrinsic clearance, a dependence of blood clearance on liver binding as well as blood binding. If, in fact, for a given drug liver binding varied much less than plasma protein or blood binding, or if a perturbation that affected blood binding had little or no effect on liver binding, R_L would be approximately proportional to f_B and (9.28) or (9.29) would be consistent with experimental evidence. Not surprisingly, there have been few studies examining the relationship between partition coefficient and clearance. Yacobi and Levy [16] studied the distribution of warfarin between serum and liver in intact rats and found that R_L averaged about 2.5, varying about twofold. However, serum protein binding in the same animals varied about tenfold and drug clearance from the serum was strongly correlated with serum protein binding ($r = 0.95$) but did not correlate with R_L ($r = 0.16$). A similar but less clear-cut situation is found with dicumarol [17], which showed an average R_L value of 0.5. Although there is a significant correlation between clearance and free fraction in serum ($r = 0.88$), there is also a significant albeit weaker correlation between clearance and R_L ($r = 0.72$).

The differentiation of (9.28), which assumes elimination rate to be a function of *total* drug concentration, from (9.26), which assumes elimination rate to be a function of *free* drug concentration, presents an unresolved dilemma because of the limited experimental work carried out to date. A conceptual dilemma also exists in that one can envision drug binding to specific proteins in the liver such as ligandin which would promote metabolism and thereby create a situation where elimination rate is a function of total drug concentration. The evidence available at this time suggests that Eq. (9.26), which is based on free drug concentration in the eliminating organ, is the more general one.

Estimates of the clearance terms required to solve the series of differential equations that characterize the physiologic pharmacokinetic model are obtained from experimental data in the species of interest. For drugs with relatively low effective intrinsic clearances, renal or biliary clearance may be measured directly by simultaneously sampling blood and urine or bile, whereas metabolic clearance may be estimated inferentially by assuming that metabolic clearance represents the difference between total clearance and the sum of renal and biliary clearances. If renal, biliary, or metabolic clearance (assuming that it occurs in a single compartment) is flow rate dependent, one must estimate the intrinsic clearance by means of an equation similar to (9.26), using experimentally determined or literature estimates of organ blood flow.

LUNG CLEARANCE

The model shown in Fig. 9.5 suggests that when the lung contributes substantially to the overall elimination of a drug, there may be difficulty in interpreting experimentally determined estimates of clearance. For example, there are examples where the total blood clearance of a drug exceeds cardiac output. This situation would appear to be prohibited by the equations developed in this chapter. One plausible explanation for this phenomenon is drug elimination in the blood itself. However, in most instances these drugs have been found to be chemically and metabolically stable in fresh whole blood or plasma. Collins et al. [18] have recently shown that clearance of a drug by the lung could result in blood clearance values that exceed total blood flow rate.

If we assume constant rate drug infusion into the right ventricle (see Fig. 9.5), at steady state the pulmonary extraction ratio E_p is given by

$$E_p = \frac{C_{in} - C_{out}}{C_{in}} \tag{9.30}$$

and

$$C_{out} = (1 - E_p)C_{in} \tag{9.31}$$

If drug were cleared only by the lung, the lung input concentration would represent a mixing of the lung output with the infused drug:

$$C_{in} = C_{out} + \frac{k_0}{Q_B} \tag{9.32}$$

where k_0 is the drug infusion rate and Q_B is equal to cardiac output. Combining Eqs. (9.31) and (9.32) and solving for C_{out}, we obtain

$$C_{out} = \frac{k_0(1 - E_p)}{Q_B E_p} \tag{9.33}$$

Drug clearance from the blood is given by the ratio of infusion rate to drug concentration in the blood at steady state. Therefore, drug clearance from arterial blood is given by

$$Cl_{art} = \frac{k_0}{C_{art}} = \frac{k_0}{C_{out}} \tag{9.34}$$

or, according to Eq. (9.33),

$$Cl_{art} = \frac{Q_B E_p}{1 - E_p} \tag{9.35}$$

It is evident from Eq. (9.35) that Cl_{art} exceeds Q_B whenever E_p exceeds 0.5, even if the lung is the sole site of drug elimination. A more general expression which takes into consideration drug elimination by other organs and tissues is as follows:

$$Cl_{art} = \frac{k_0}{C_{out}} = \frac{Q_B E_p}{1 - E_p} + \sum Q_t E_t \tag{9.36}$$

where Q_t is the blood flow rate to an eliminating tissue and E_t is the drug extraction ratio for that tissue.

The preceding analysis applies strictly only when drug concentration is measured in arterial blood or plasma [18]. Drug concentration in venous blood may be substituted only if there is no elimination in tissues drained by the vein that is sampled. Although this substitution may be valid for many drugs, uncertainty must prevail for any drug that is subject to extrahepatic nonrenal elimination. For the case of sampling from a vein that drains eliminating tissue, the steady-state drug concentration is given by

$$C_{ven} = (1 - E_t)C_{art} \tag{9.37}$$

where E_t is the drug extraction ratio of the eliminating tissue. It follows from Eq. (9.34) that

$$C_{ven} = \frac{(1 - E_t)k_0}{Cl_{art}} \tag{9.38}$$

Since drug clearance from venous blood is given by k_0/C_{ven}, it follows that

$$Cl_{ven} = \frac{Cl_{art}}{1 - E_t} \tag{9.39}$$

Thus in the absence of elimination by the local tissue which is drained by the sampling vein, $Cl_{ven} = Cl_{art}$. In any case, Cl_{ven} will always be greater than or equal to Cl_{art}. Therefore, whether blood is sampled from the venous or arterial side, clearance can exceed cardiac output if pulmonary elimination is significant.

APPARENT VOLUME OF DISTRIBUTION

The apparent volume of distribution at steady state for a drug is a function of the anatomical volume into which it distributes as well as the degree of binding in blood and extravascular tissues. For the model shown in Fig. 9.3A, the apparent volume of distribution is given by

$$V = V_B + R_L V_L + R_M V_M \tag{9.40}$$

or

$$V = V_B + \frac{f_B V_L}{f_L} + \frac{f_B V_M}{f_M} \tag{9.41}$$

For the general case

$$V = V_B + \sum R_t V_t \tag{9.42}$$

or

$$V = V_B + f_B\left(\sum \frac{V_t}{f_t}\right) \tag{9.43}$$

Benowitz et al. [13] have demonstrated for lidocaine in the monkey that the pharmacokinetically derived volume of distribution at steady state V_{ss} (see Chap. 5) is equivalent to the sum of the products of tissue masses (volumes) and equilibrium distribution ratios (R values) as indicated in Eq. (9.42).

NONLINEAR DISPOSITION

In the absence of specific information to the contrary, we usually assume that drug elimination is a linear process and introduce a single clearance term in the mass-balance rate equation for the body regions capable of elimination [see Eq. (9.16) or (9.18)]. However, at sufficiently high doses, enzyme-mediated processes such as drug metabolism, renal tubular secretion, or biliary secretion may require concentration-dependent clearance terms to describe the time course of drug in each body region. Assuming that drug metabolism in the liver is described by Michaelis-Menten kinetics, one must rewrite (9.16) as follows:

$$V_L \frac{dC_L}{dt} = Q_L\left(C_B - \frac{C_L}{R_L}\right) - \frac{V_m C_L'}{K_m' + C_L'} \tag{9.44}$$

where C_L and C_L' are the total and free drug concentrations in liver, respectively; V_m is the maximum rate of elimination (mass units/time units) from the liver; and K_m' is the Michaelis constant (concentration units) with respect to free drug. The ratio of V_m to K_m' is equal to Cl_L', the intrinsic clearance with respect to free drug concentration in the liver.

Estimates of V_m and K_m may be obtained from in vivo pharmacokinetic data (see Chap. 7). Some investigators have successfully estimated values for V_m and K_m from in vitro enzyme kinetic data [19–21].

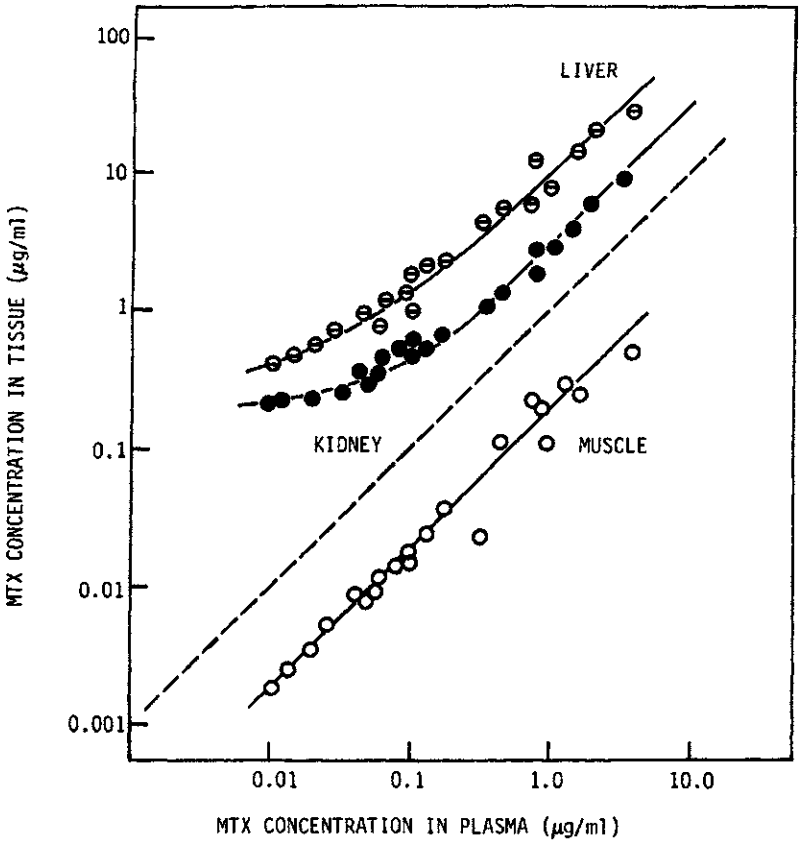

Fig. 9.6 Relative distribution of methotrexate (MTX) between plasma and muscle, kidney, or liver in the mouse following intravenous doses of 0.1, 0.3, and 3 mg/kg. Drug concentrations were determined at times ranging from 5 to 120 min following injection. During the period of observation a unique relationship exists between drug concentration in the plasma and the concentration in each of these three tissues. Distribution into the muscle is linear and apparently limited to the extracellular space. At high drug concentrations in plasma, distribution into both kidney and liver is linear, but the drug is concentrated in these organs to the extent of about 3:1 and 10:1, respectively. At low drug concentrations in plasma, concentrations in these tissues appear to approach constant values presumed to be associated with strong binding of methotrexate to dihydrofolate reductase. (From Ref. 22, reprinted with permission of the author.)

Drug binding to plasma proteins and tissue components is usually assumed to be linear and effectively accounted for by introducing an R value in the mass-balance rate equation. This simplification, however, may not always be appropriate. In the case of methotrexate [22], tissue-to-blood partition coefficients show a marked concentration dependence, at least in some tissues (see Fig. 9.6). This is believed to be the result of strong binding of the drug to dihydrofolate reductase in the tissue. In this case, in vivo binding isotherms consist of a linear and a saturable term. Drug concentration in tissue is given by

$$C_t = R_t C_B + \frac{aC_B}{E + C_B} \tag{9.45}$$

where a is the strong binding constant and E is the dissociation constant [22]. At high methotrexate concentrations the second term of (9.45) is negligible and binding is approximately linear. A similar approach has been suggested to handle nonlinear plasma protein binding [23].

MEMBRANE-LIMITED MODELS

Physiologic-pharmacokinetic studies with certain drugs, including methotrexate [22], tetraethylammonium ion [24], and actinomycin D [6], have revealed tissue uptake characteristics that are not consistent with a blood flow rate-limited distribution process. For example, the declining concentrations of actinomycin D in dog testes do not parallel the declining drug concentrations in plasma after a rapid intravenous injection (see Fig. 9.7). Figure 9.8 shows methotrexate concentrations determined simultaneously in plasma and bone marrow of the rat at several doses and clearly reveals that no unique relationship exists for the methotrexate tissue-to-blood ratios, unlike the situation described in Fig. 9.6. At a given methotrexate concentration in plasma, (e.g., 0.1 μg/ml), there are different concentrations in bone marrow, depending on the dose administered and the time the tissue sample was taken. These data indicate that the bone marrow is not a blood flow rate-limited equilibrium compartment and suggest a membrane-limited transport. Similar results have been found with respect to tumor uptake of methotrexate in spontaneous canine lymphosarcoma [25].

Figure 9.9 is a scheme for a body region where membrane-limited transport prevails. The model assumes that all concentrations represent free drug concentrations. Exchange across the capillary membrane is probably so rapid that the blood and interstitial fluid may be assumed to form one equilibrium compartment, termed the extracellular space. For the extracellular compartment the mass-balance rate equation is

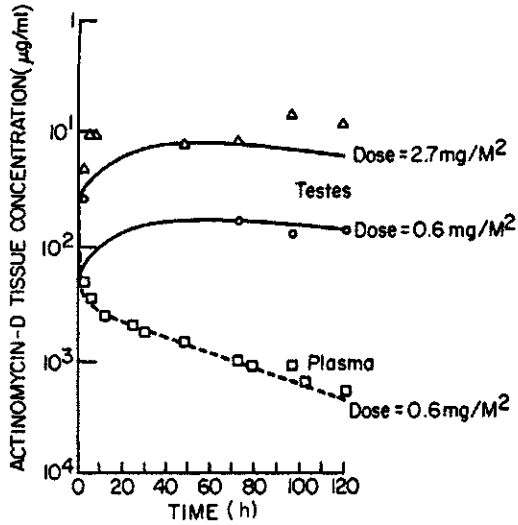

Fig. 9.7 Actinomycin-D concentrations in plasma and testes following a 0.6 mg/m^2 intravenous dose, and in testes following a 2.7 mg/m^2 intravenous dose, in the beagle dog. Drug concentrations in testes do not parallel the declining plasma curve. Simulations that assume cellular membrane resistance (solid lines) are in reasonable agreement with the tissue data. [From Ref. 6, © 1977 American Society for Pharmacology and Experimental Therapeutics, The Williams and Wilkins Company (agent).]

$$V_E \frac{dC'_E}{dt} = Q_i(C'_B - C'_E) - \text{net flux} \tag{9.46}$$

where V_E is the extracellular space (sum of capillary blood and interstitial fluid volume), C'_E is the free drug concentration in the extracellular space, Q_i is the blood flow rate to the region, and C'_B is free drug concentration in the blood pool. The mass-balance rate equation for the intracellular space is

$$V_I \frac{dC'_I}{dt} = \text{net flux} \tag{9.47}$$

where V_I and C'_I are the volume and free drug concentration, respectively, of the intracellular fluid.

Net flux (transport) may be assumed preliminarily to be diffusive but in some cases must be handled as a saturable, facilitated process demonstrating Michaelis-Menten kinetics. In the case of diffusive transport, which appears to apply to actinomycin D uptake in dog testes [6], net flux is given by the equation

$$\text{net flux} = K_i(C'_E - C'_I) \tag{9.48}$$

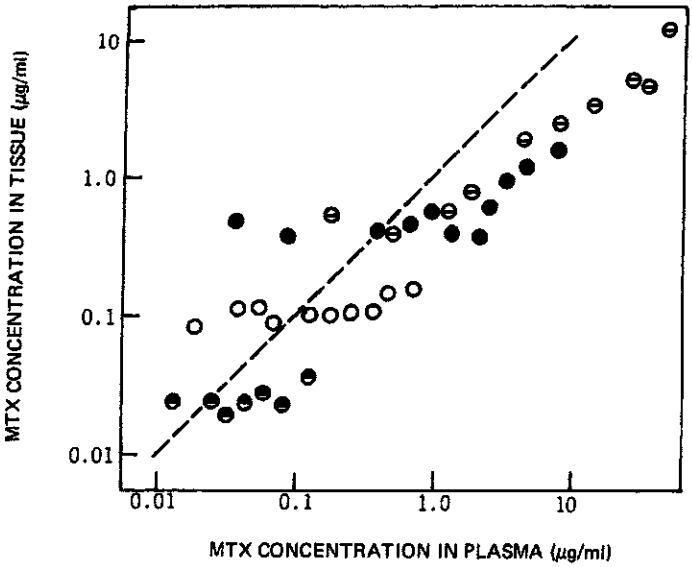

Fig. 9.8 Relative distribution of methotrexate (MTX) between plasma and bone marrow in the rat following intravenous doses of 0.05 (⊖), 0.25 (○), 2.5 (●), and 25 (⊖) mg/kg. Unlike the situation described in Fig. 9.6, no unique thermodynamic relationship is seen between drug in tissue and that in plasma. The dependence of drug concentration in tissue on dose as well as on drug concentration in plasma suggests a model that includes membrane resistance to transport. (From Ref. 22, reprinted with permission.)

where K_i is the effective membrane permeability coefficient. Membrane resistance to drug transport is limiting only if the diffusion parameter K_i is much smaller than the tissue perfusion rate per unit volume [6].

Studies with methotrexate [22] and tetraethylammonium ion [24] suggest that the assumption of simple diffusive transport is not sufficient to describe membrane-limited uptake of these drugs into certain tissues. These uptake data have been rationalized by expressing net flux as a concentration-dependent term:

$$\text{net flux} = \frac{V_m C'_E}{K'_m + C'_E} - \frac{V_m C'_I}{K'_m + C'_I} + K_i(C'_E - C'_I) \qquad (9.49)$$

where V_m is the maximum facilitated transport rate and K'_m is the Michaelis constant with respect to unbound drug. It is assumed that the efflux and influx of the facilitated process are characterized by the same parameters (i.e., membrane transport is symmetric). It is of interest to note that for both drugs the passive permeability term $K_i(C'_E - C'_I)$ was assumed to be negligible for the doses used. Mintum

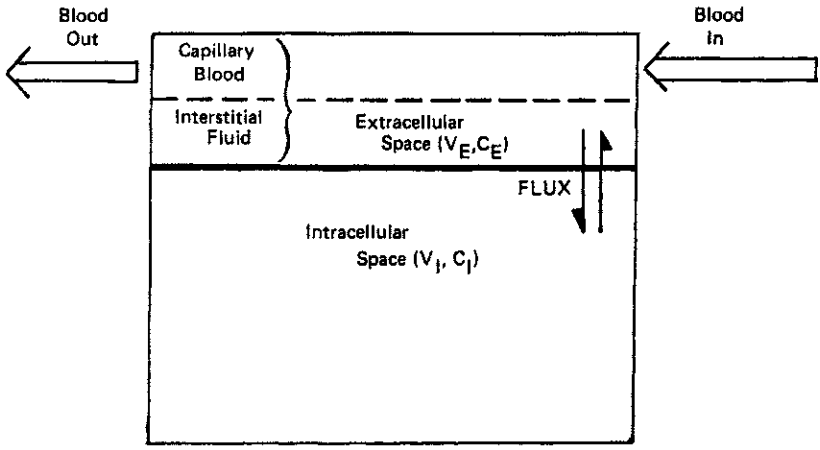

Fig. 9.9 Schematic representation of a tissue region in a physiological pharmacokinetic model which assumes membrane resistance. For most drugs the capillary membrane is very permeable, diffusion to the interstitial fluid is very fast, and the plasma and interstitial fluid can be combined into one equilibrium space termed the extracellular space. The volume of and drug concentration in this space are designated V_E and C_E, respectively. For some drugs the uptake rate (flux) by the cell is limited by the resistance of the membrane to drug transport. The volume of and drug concentration in the intracellular space are designated V_I and C_I, respectively.

et al. [24] have described the use of total rather than free drug concentrations for membrane-limited models.

The incorporation of *both* nonlinear binding and facilitated membrane-limited transport into a physiological pharmacokinetic model is a more formidable task but has been required and successfully accomplished in the case of methotrexate [22,26].

SPECIES SIMILARITY AND SCALE-UP

The development of a detailed physiological pharmacokinetic model for a drug in humans is a very difficult proposition. The almost insurmountable barrier is the vast amount and array of data needed to validate the model, particularly the need for tissue concentration data. Limited tissue-to-blood partition coefficient data for certain drugs in humans are available from studies conducted during surgery or on necropsy, but the reliability of these data as well as their applicability to general populations are suspect. Thus we must often rely substantially on in vitro or animal studies supplemented by clinical pharmacokinetic studies.

Table 9.2 Relationship Between Certain Physiological or Anatomical Properties and Body Weight Among Mammals

Property	Exponent
Creatinine clearance	0.69
Inulin clearance	0.77
PAH clearance	0.80
Basal O_2 consumption	0.73
Endogenous N output	0.72
O_2 consumption by liver slices	0.77
Kidney weight	0.85
Heart weight	0.98
Liver weight	0.87
Stomach and intestines weight	0.94
Blood weight	0.99

Note: Data from different species were fitted to the following equation: property = (body weight)$^{\text{exponent}}$. (From Ref. 28.)

Dedrick and Bischoff [27] have noted: "There are many similarities in the anatomy and physiology of mammalian species. A general belief in this similarity has been the cornerstone of most biomedical research. We share a remarkable geometric similarity. The same blood flow diagram could be used for all mammals, and most organs and tissues are similar fractions of the body weight. Major qualitative differences, such as the absence of a gall bladder in some species, are the exception." Adolph [28] observed that many anatomical and physiological variables can be correlated among mammals as exponential functions of body weight. Some examples are presented in Table 9.2. The anatomical variables are more nearly proportional (as indicated by an exponent of unity) to body weight than are the metabolic or physiological properties. Generally, physiologic function per unit of organ weight or per unit of animal weight decreases as size increases. Bischoff et al. [11] have presented scaling graphs for certain organ blood flow rates (specifically, kidney, liver, and muscle) as a function of body weight (see Fig. 9.10). Edwards [29] has found excellent correlations for renal processes (including inulin clearance, PAH clearance, renal blood flow, creatinine clearance, and daily urine output) among mammals as exponential functions of body weight (see Fig. 9.11). The values of the exponents were in the order of 0.7 to 0.8. Edwards also suggests that renal blood flow is generally 26% of cardiac

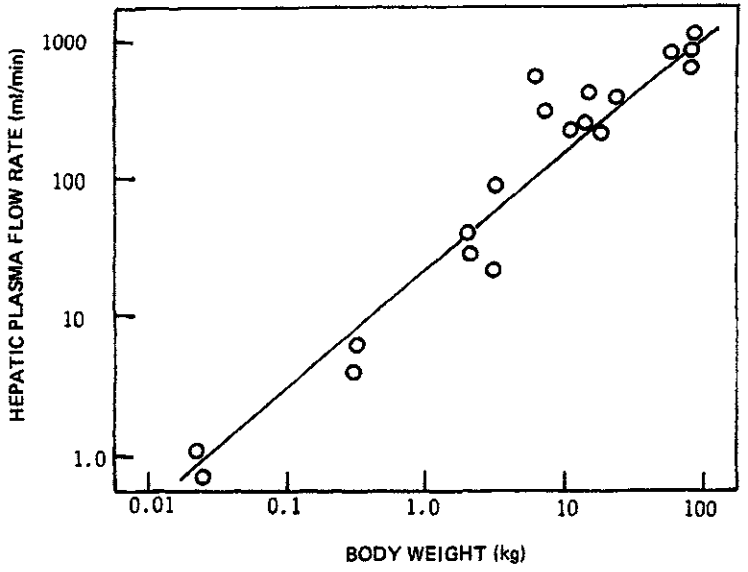

Fig. 9.10 Relationship between hepatic plasma flow rate and total body weight in several animal species. (Data from Ref. 11.)

output in mammals, independent of body weight. In this respect, renal blood flow differs from hepatic portal blood flow, which represents a relatively greater proportion of cardiac output in larger species [29].

If drug distribution involved purely physical interactions between xenobiotics and biological tissues or fluids, it might be expected to follow principles of thermodynamic partitioning with relatively minor interspecies variation. An equilibrium distribution ratio (R value) determined for a given tissue in a laboratory animal might then be useful for a model to be applied to humans. This seems to be a plasusible idea for certain fat-soluble compounds, including dieldrin [30], thiopental [31], and kepone [32], but less encouraging results have been found for other compounds such as methotrexate [11] and digoxin [8,10]. At this time more work needs to be done to examine the merits of this hypothesis. It is reasonable to suggest that even a preliminary interest in this approach requires as a minimum that V_{ss} values for the drug be rather similar in the two or more species. This comparability is not sufficient but it is necessary. There has been some interest in using in vitro data to estimate in vivo binding parameters [31].

The most significant species differences that may confound pharmacokinetic predictability are in the pathways and kinetic characteristics of metabolism. Although humans usually metabolize drugs less rapidly then other animal species that are commonly used in drug development studies, and microsomal enzyme activities per kilogram of

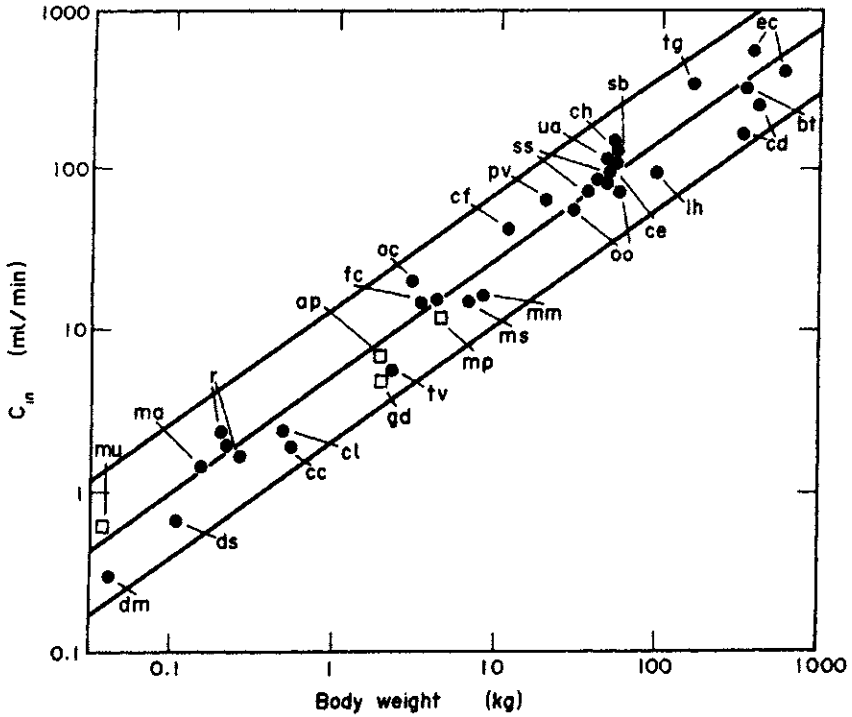

Fig. 9.11 Relationship between inulin clearance C_{in} and total body weight for mammals (●) and for four species of birds (□) $C_{in} = 5.359\ BW^{0.72}$. The key to species is provided in Ref. 29. (From Ref. 29.)

body weight tend to decrease as body weight increases, many exceptions exist. Quite different metabolic pathways may dominate in different species and toxicity may sometimes correlate with the concentration of a reactive intermediate that represents only a minor elimination pathway.

On the other hand, there is increasing evidence that metabolic information from in vitro systems may be used for quantitative parameter estimation in pharmacokinetic models. These in vitro systems have included both crude and purified enzyme preparations, other cell extracts such microsomes, cell suspensions, tissue slices, and isolated organs. Dedrick and Bischoff [27] propose that it should be possible to use metabolism data from properly designed in vitro systems in conjunction with pharmacokinetic models to provide a basis for predicting pharmacokinetic behavior of xenobiotics in any mammalian species, including humans. They have recently reviewed the evidence in support of this hypothesis. The most notable in vitro-

Table 9.3 Comparison of Extraction Ratios Predicted from In Vitro Estimates of V_m and K_m, and Observed in Isolated Perfused Rat Liver

Drug	V_m/K_m ml/ min (g liver)$^{-1}$	K_m (mM)	Extraction Ratio	
			Predicted	Observed
Alprenolol	23.5	0.017	0.92	>0.90
Propranolol	10.0	0.005	0.83	>0.90
Lidocaine	8.2	0.058	0.80	>0.90
Phenytoin	2.0	0.031	0.50	0.53
Hexobarbital	1.6	0.105	0.44	0.33
Carbamazepine	0.11	0.73	0.05	0.04
Antipyrine	0.08	22.0	0.04	0.01

Source: From Ref. 19.

in vivo correlations have been observed by Rane et al. [19]. The results of their comparison of observed hepatic extraction ratios with those calculated from V_{max}/K_m ratios obtained from rat liver preparations are summarized in Table 9.3.

Probably the most fascinating approach to interspecies correlation of drug concentration data has been offered by Dedrick et al. [33] with methotrexate. This analysis is empirical and perhaps limited to a few compounds but is nevertheless interesting, informative, and exciting. Figure 9.12 shows methotrexate concentrations in plasma or serum after injection of various doses to different animal species, including the mouse, rat, monkey, dog, and humans. The range of variables is as follows: body weight, 22 to 70,000 g (ratio of 3000 to

Table 9.4 Equivalent Times for Several Species

Species	Average Body Weight (g)	Body Weight$^{1/4}$ ($g^{1/4}$)	Equivalent Time (min)
Mouse	22	2.16	0.13
Rat	160	3.56	0.22
Monkey	4,000	7.95	0.49
Dog	5,000	8.42	0.52
Humans	70.000	16.3	1.00

Source: From Ref. 33.

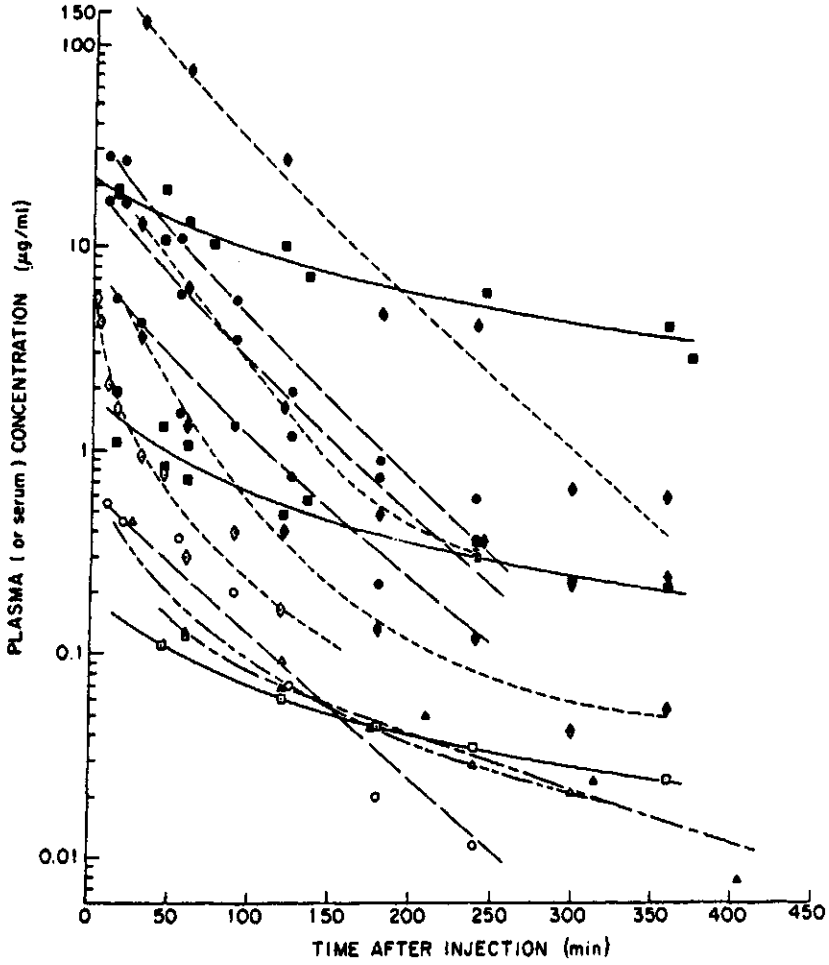

Fig. 9.12 Plasma (or serum) concentration of methotrexate after intravenous or intraperitoneal injection of different doses. The species are indicated by diamonds (mice), circles (rats), closed triangles (monkey), open triangles (beagle dog), and squares (humans). (Data from Ref. 33.)

1); dose per unit body weight, 0.1 to 450 mg/kg (4500 to 1); and methotrexate concentrations in plasma or serum, 0.0077 to 130 μg/ml (17,000 to 1).

An attempt was made to represent all the data by a single curve. Normalization of the ordinate in Fig. 9.12 was achieved by dividing observed drug concentrations by the dose per unit body weight. Such normalization implicitly assumes linear relationships among rele-

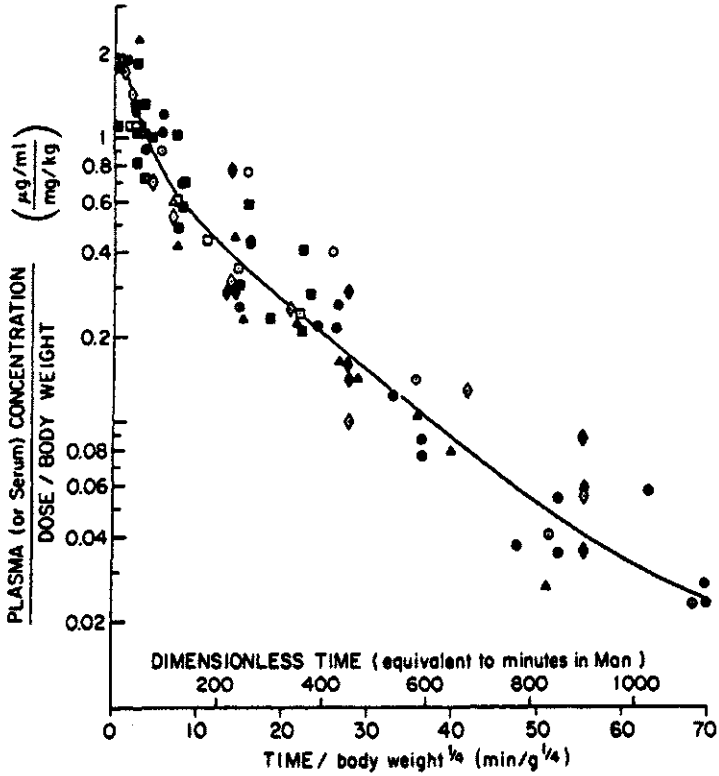

Fig. 9.13 Correlation of methotrexate concentration data in plasma (or serum) in mouse, rat, monkey, dog, and humans. Symbols are as indicated in Fig. 9.12. (From Ref. 33.)

vant thermodynamic phenomena such as equilibrium distribution in major tissues. It would not be expected to apply to a drug that is strongly and nonlinearly bound to proteins or other macromolecules. These assumptions may be reasonably applied to methotrexate for some time after injection (when concentrations are high), but are inappropriate at later times.

Normalization of the abscissa in Fig. 9.12 requires introduction of an interesting kinetic concept. It is evident that changes are taking place more rapidly in the smaller animals than in the larger animals. Dedrick et al. [33] developed the idea of *equivalent time* to account for these kinetic differences. For example, since the decline of methotrexate concentrations in plasma or serum occurs about an order of magnitude faster in the mouse than in humans, an equivalent time might be the mean residence time of the vascular system or the ratio of blood volume to cardiac output. The latter has a value of about

1 min in humans and varies as a function of body weight to the 0.2 power. In the case of methotrexate concentrations, Dedrick and coworkers chose to use an empirical function of body weight (i.e., to normalize the abscissa by dividing time by body weight raised to the 0.25 power). Table 9.4 shows the correspondence between the fourth root of weight and an equivalent time based on unity for humans.

The correlation developed in this manner is shown in Fig. 9.13. All data from Fig. 9.12 have been included up to a time parameter of 70 ($min/g^{1/4}$). Accordingly, mouse data beyond 150 min and rat data beyond 250 min are not included. Agreement is very good and variations appear to be principally random. The application of this approach to other drugs that demonstrate linear pharmacokinetics and are essentially excreted unchanged is a distinct possibility; the success of this approach for drugs that are substantially metabolized is probably unlikely.

The development, validation, and application of physiologic pharmacokinetic models is a very exciting area of research. A great deal of credit must be accorded to Bischoff and Dedrick for their pioneering effort and prolific contributions. In all its ramifications, this pharmacokineric approach offers the possibility of unusual insight into complex biological systems.

REFERENCES

1. K. J. Himmelstein and R. J. Lutz. A review of the applications of physiologically based pharmacokinetic modeling. *J. Pharmacokinet. Biopharm.* *7*:127 (1979).
2. N. Benowitz, R. P. Forsyth, K. L. Melmon, and M. Rowland. Lidocaine disposition kinetics in monkey and man: II. Effects of hemmorrhage and sympathomimetic drug administration. *Clin. Pharmacol. Ther.* *16*:99 (1974).
3. R. L. Dedrick. Animal scale-up. *J. Pharmacokinet. Biopharm.* *1*:435 (1973).
4. K. B. Bischoff. Some fundamental considerations of the applications of pharmacokinetics to cancer chemotherapy. *Cancer Chemother. Rep.* *59*:777 (1975).
5. M. Rowland, L. Z. Benet, and G. G. Graham. Clearance concepts in pharmacokinetics. *J. Pharmacokinet. Biopharm.* *1*:123 (1973).
6. R. J. Lutz, W. M. Galbraith, R. L. Dedrick, R. Shrager, and L. B. Mellett. A model for the kinetics of distribution of actinomycin-D in the beagle dog. *J. Pharmacol. Exp. Ther.* *200*:469 (1977).
7. F. G. King and R. L. Dedrick. Pharmacokinetic model for 2-amino-1,3,4-thiadiazole in mouse, dog, and monkey. *Cancer Treat. Rep.* *63*:1939 (1979).

8. L. I. Harrison and M. Gibaldi. Physiologically based pharmacokinetic model for digoxin disposition in dogs and its preliminary application to humans. *J. Pharm. Sci.* *66*:1679 (1977).
9. A. Tsuji, E. Miyamoto, T. Terasaki, and T. Yamana. Physiological pharmacokinetics of β-lactam antibiotics: Penicillin V distribution and elimination after intravenous administration in rats. *J. Pharm. Pharmacol.* *31*:116 (1979).
10. L. I. Harrison and M. Gibaldi. Physiologically based pharmacokinetic model for digoxin distribution and elimination in the rat. *J. Pharm. Sci.* *66*:1138 (1977).
11. K. B. Bischoff, R. L. Dedrick, D. S. Zaharko, and J. A. Longstreth. Methotrexate pharmacokinetics. *J. Pharm. Sci.* *60*:1128 (1971).
12. K. B. Bischoff, R. L. Dedrick, and D. S. Zaharko. Preliminary model for methotrexate pharmacokinetics. *J. Pharm. Sci.* *59*:149 (1970).
13. N. Benowitz, R. P. Forsyth, K. L. Melmon, and M. Rowland. Lidocaine disposition kinetics in monkey and man: I. Prediction by perfusion model. *Clin. Pharmacol. Ther.* *16*:87 (1974).
14. H-S. G. Chen and J. F. Gross. Estimation of tissue-to-plasma partition coefficients used in physiological pharmacokinetic models. *J. Pharmacokinet. Biopharm.* *7*:117 (1979).
15. G. R. Wilkinson and D. G. Shand. A physiological approach to hepatic drug clearance. *Clin. Pharmacol. Ther.* *18*:377 (1975).
16. A. Yacobi and G. Levy. Comparative pharmacokinetics of coumarin anticoagulants: XIV. Relationship between protein binding, distribution and elimination kinetics of warfarin in rats. *J. Pharm. Sci.* *64*:1660 (1975).
17. G. Levy, C.-M. Lai, and A. Yacobi. Comparative pharmacokinetics of coumarin anticoagulants: XXXII. Interindividual differences in binding of warfarin and dicumarol in rat liver and implications for physiological pharmacokinetic modeling. *J. Pharm. Sci.* *67*:229 (1978).
18. J. M. Collins, R. L. Dedrick, F. G. King, J. L. Speyer, and C. E. Myers. Nonlinear pharmacokinetic models for 5-fluorouracil in man: Intravenous and intraperitoneal routes. *Clin. Pharmacol. Ther.* *28*:235 (1980).
19. A. Rane, G. R. Wilkinson, and D. G. Shand. Prediction of hepatic extraction ratio from in vitro measurement of intrinsic clearance. *J. Pharmacol. Exp. Ther.* *200*:420 (1977).
20. R. L. Dedrick, D. D. Forrester, and D. H. W. Ho. In vitro-in vivo correlation of drug metabolism—deamination of 1-β-D-arabinofuranosylcytosine. *Biochem. Pharmacol.* *21*:1 (1972).
21. R. L. Dedrick and D. D. Forrester. Blood flow limitations in interpreting Michaelis constant for ethanol oxidation in vivo. *Biochem. Pharmacol.* *22*:1133 (1973).

22. R. L. Dedrick, D. S. Zaharko, and R. J. Lutz. Transport and binding of methotrexate in vivo. *J. Pharm. Sci.* *62*:882 (1973).
23. D. S. Greene, R. Quintiliani, and C. H. Nightingale. Physiological perfusion model for cephalosporin antibiotics: I. Model selection based on blood concentrations. *J. Pharm. Sci.* *67*:191 (1978).
24. M. Mintum, K. J. Himmelstein, R. L. Schroder, M. Gibaldi, and D. D. Shen. Tissue distribution kinetics of tetraethylammonium ion in the rat. *J. Pharmacokinet. Biopharm.* *8*:373 (1980).
25. R. J. Lutz, R. L. Dedrick, J. A. Straw, M. M. Hart, P. Klubes, and D. S. Zaharko. The kinetics of methotrexate distribution in spontaneous canine lymphosarcoma. *J. Pharmacokinet. Biopharm.* *3*:77 (1975).
26. K. H. Yang, W. P. Fung, R. J. Lutz, R. L. Dedrick, and D. S. Zaharko. In vivo methotrexate transport in murine Lewis lung tumor. *J. Pharm. Sci.* *68*:941 (1979).
27. R. L. Dedrick and K. B. Bischoff. Species similarity in pharmacokinetics. *Fed. Proc.* *39*:54 (1980).
28. E. F. Adolph. Quantitative relations in the physiological constitutions of mammals. *Science* *109*:579 (1949).
29. N. A. Edwards. Scaling of renal functions in mammals. *Comp. Biochem. Physiol.* [A] *52*:63 (1975).
30. C. G. Hunter, J. Robinson, and M. Roberts. Pharmacodynamics of dieldrin (HEOD): Ingestion by human subjects for 18 to 24 months and post-exposure for eight months. *Arch. Environ. Health* *18*:12 (1969).
31. K. B. Bischoff and R. L. Dedrick. Thiopental pharmacokinetics. *J. Pharm. Sci.* *57*:1346 (1968).
32. P. M. Bungay, R. L. Dedrick, and H. B. Matthews. Pharmacokinetics of halogenated hydrocarbons. *Ann. N.Y. Acad. Sci.* *320*:257 (1979).
33. R. L. Dedrick, K. B. Bischoff, and D. S. Zaharko. Interspecies correlation of plasma concentration history of methotrexate. *Cancer Chemother. Rep.* *54*:95 (1970).